Received April 4, 2019, accepted April 22, 2019, date of publication May 1, 2019, date of current version May 6, 2019.

Digital Object Identifier 10.1109/ACCESS.2019.2913314

Design of High-Selectivity Asymmetric Three-Way Equal Wideband Filtering Power Divider

CHUANMING ZHU AND JIAN ZHANG
School of Electronics and Information, Hangzhou Dianzi University, Hangzhou 310018, China
Corresponding author: Jian Zhang (zhangjian@hdu.edu.cn)

ABSTRACT An asymmetric three-way equal wideband filtering power divider with high selectivity is presented in this paper. The proposed three-way filtering power divider is an asymmetric structure which is composed of two different λ/4 transformers, a pair of short-ended parallel coupled lines, an open-ended parallel coupled line, and a three-line parallel coupled line. Based on 2:1 unequal Wilkinson power divider, an equal three-way power divider is obtained with energy subdivided by three-line parallel coupled line. Subsequently, a Wilkinson power divider with the wideband filtering response is realized by adding a pair of short-ended parallel coupled lines that can provide multiple transmission zeros and poles. Presented with an equivalent circuit, the design procedure for asymmetric three-way equal filtering power divider is developed. Moreover, the reasons for and associated measures of large magnitude imbalance are also analytically developed. The measured results show that the proposed filtering power divider has more than 57.3% 1-dB fractional bandwidth, less than 0.4 dB insertion losses, better than 19.5 dB return loss, and more than 14.9 dB isolation from direct current to 3.3 GHz.

INDEX TERMS Three-way, filtering power divider, high-selectivity, wideband.

I. INTRODUCTION

Recently, filtering power dividers (FPDs) that integrate Wilkinson power divider (WPD) and bandpass filter (BPF) into a single circuit have attracted our interests. Many efforts have been conducted to develop FPDs, such as the ability to realize compact size [1], to perform wide stopband [2], to achieve arbitrary power division ratio [3], [4], to obtain single-ended-to-balanced [5], and to perform reconfigurable function [6], [7]. All these even-way FPDs have good performances. However, it is difficult to design FPDs with odd-number of output ports. For example, when the number of its output ways becomes three, it will increase the difficulty in design and fabrication, such as the inevitable stray couplings between resonators and 3-D floating common node connecting three pairs of isolation components.

So far, a lot of three-way Wilkinson power dividers (WPDs) [8]–[16] have been published. Based on the even-way WPD, the method of recombining power of two output ports into one [8], [9], or subdividing power of one port into two [10]–[12] can realize one three-way WPD. The other way is to symmetrically divide signal into three output ports [13]–[18], and an equal three-way WPD can be also achieved.

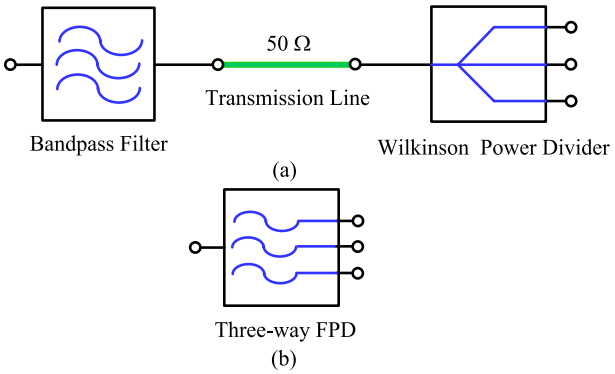

FIGURE 1. (a) Topology of conventional cascaded BPF, TL, and three-way WPD, (b) Topology of three-way FPD.

As shown in Fig. 1(a), in the feeding network of antennas, bandpass filter is sometimes cascaded with three-way WPD, which may lead large circuit size and more insertion losses (ILs). As shown in Fig. 1(b), if BPF is integrated into three-way WPD, above problems will be solved. Then a symmetric three-way equal FPD [19] is obtained by replacing λ/4 transformers of conventional WPD with multiple

The associate editor coordinating the review of this manuscript and approving it for publication was Haiwen Liu.

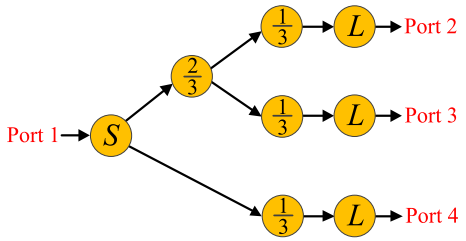

FIGURE 2. Design concept of proposed three-way wideband FPD.

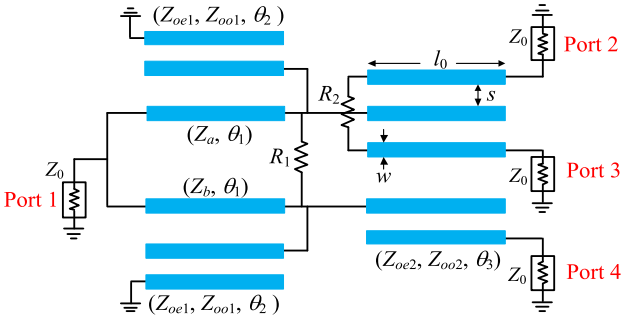

FIGURE 3. Schematic diagram of proposed asymmetric three-way wideband FPD.

coupled lines. Nevertheless, its skirt selectivity [19] needs to be improved.

In this paper, a high-selectivity asymmetric three-way equal wideband FPD is proposed. Based on 2:1 unequal WPD, a three-way FPD is realized using the short-ended parallel coupled lines (PCLs) and three-line PCL. Theoretical analysis for asymmetric three-way FPD is discussed, while the parameters of three-way FPD are analytically determined. The proposed three-way wideband FPD is fabricated on the substrate Rogers RT6010 ($\varepsilon_{\rm re} = 10.2$, $h = 1.27$ mm, and $\tan\delta = 0.0023$). Detailed design and measured results are discussed as follows.

II. THREE-WAY FILTERING POWER DIVIDER DESIGN

A. STRUCTURE

Fig. 2 shows the design concept of three-way wideband FPD. In Fig. 2, the input energy is firstly divided into 1/3 and 2/3, and then the part of 2/3 is subdivided into 1/3 and 1/3. Thus three output ports of three-way PD can have the equal power. Fig. 3 gives the schematic diagram of the proposed asymmetric three-way equal wideband FPD. It is consisted of two λ/4 transformers (Z_a, θ_1) and (Z_b, θ_1), a pair of short-ended PCLs (Z_{oe1}, Z_{oo1}, θ_2), one open-ended PCLs (Z_{oe2}, Z_{oo2}, θ_3), and one three-line PCL (w, l_0, s). A pair of short-ended PCLs can realize multiple transmission zeros (TZs) and poles, and thus a wideband filtering response can be achieved. An isolation resistor R_1 is added between two λ/4 transformers to realize the matching and isolation between ports i ($i = 2, 3$) and 4. R_2 is added onto the open-ended of three-line PCL to achieve matching and isolation between port 2 and 3.

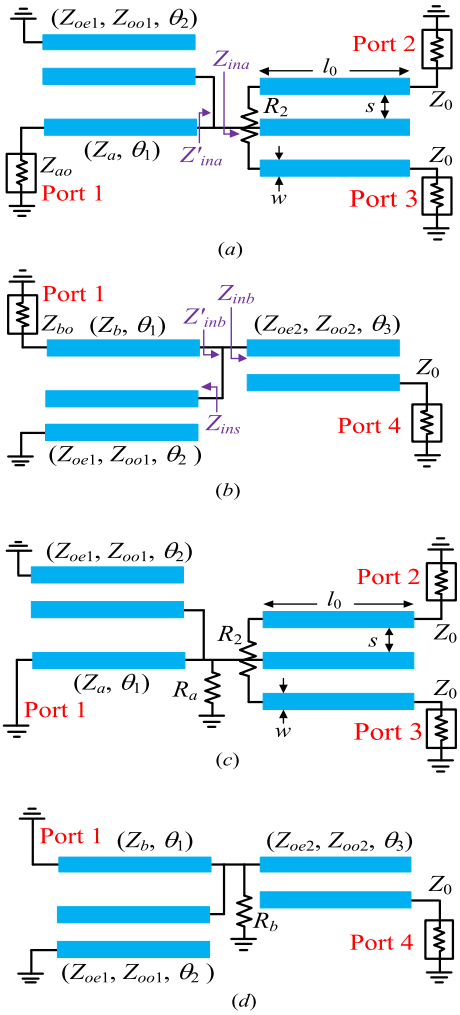

FIGURE 4. Decomposing of proposed circuit in Fig. 2. (a) even-mode circuit for Arm-a. (b) even-mode circuit for Arm-b. (c) odd-mode circuit for Arm-a. (d) odd-mode circuit for Arm-b.

B. ANALYSIS OF EVEN-AND ODD-MODE CIRCUIT

By applying the even-mode excitation, the simplified equivalent circuits are obtained, as shown in Figs. 4(a) and (b). For the matching at port 1, the terminal impedances (Z_{ao}, Z_{bo}) and the parameters (Z_a, Z_b) can be derived as [20]:

$$Z_{ao} = Z_0\left(1+k^2\right)/k^2 \tag{1a}$$

$$Z_{bo} = Z_0\left(1+k^2\right) \tag{1b}$$

$$Z_a = Z_0\sqrt{\left(1+k^2\right)/k^3} \tag{1c}$$

$$Z_b = Z_0\sqrt{k\left(1+k^2\right)} \tag{1d}$$

where the power sum of port 2 and 3 are k^2 times of power of port 4. Z_a and Z_b are the characteristic impedance of λ/4 transformers of arm-a and arm-b, respectively. Figs. 4(c) and (d) give its odd-mode equivalent circuits. To realize good matching at port 1 and isolation between port 2 (or 3) and port 4, the resistor R_a for arm-a and R_b for

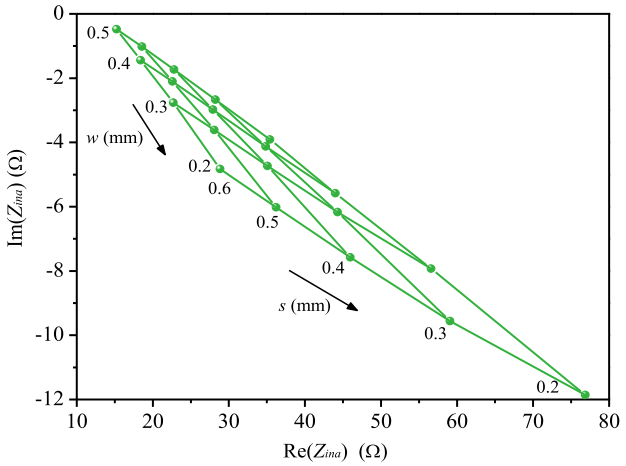

FIGURE 5. Extracted Z_{ina} against w and s.

arm-b can be obtained as:

$$R_a = Z_0/k \tag{2a}$$
$$R_b = kZ_0 \tag{2b}$$

Then R_1 is calculated as $R_a + R_b$. Herein, the loaded short-ended PCLs are firstly not considered. To realize perfect matching [21], [22], the input impedance Z_{ina} and Z_{inb} in Figs. 4(a) and (b) need to be equal to R_a and R_b, respectively. The design formula for three-line PCL is extremely complicated [23], the microstrip physical model (w, l_0, s) is employed for design simplicity. Fig. 5 shows the extracted input impedance Z_{ina} against w and s. The desired real and imaginary part of Z_{ina} can be realized by properly choosing w and s from Fig. 5.

As shown in Fig. 4(b), Z_{inb} are calculated as:

$$Z_{inb} = \frac{mZ_0 \sin 2\theta_3 + j(n^2 + m^2 \cos^2 \theta_3)}{m \sin 2\theta_3 + j4Z_0 \sin^2 \theta_3} \tag{3}$$

where $m = Z_{oe2} + Z_{oo2}$, $n = Z_{oe2} - Z_{oo2}$. Based on above equations (1)-(3), the initial parameters are obtained as: $Z_0 = 50\ \Omega, Z_a = 51.5\ \Omega, Z_b = 103\ \Omega, Z_{oe2} = 140\ \Omega, Z_{oo2} = 21\ \Omega$, $R_1 = 106\ \Omega$, $w = 0.33$ mm, $s = 0.36$ mm, $l_0 = 21.1$ mm, $\theta_1 = \theta_3 = 90°$ at $f_0 = 1.5$ GHz. R_2 are initially chosen as 160 Ω since it has no effects on transmission coefficients that are firstly designed. The design of R_2 will be introduced in the behind sections.

Figs. 6(a) and (b) show the theoretic response without short-ended PCLs. Within the passband, less than 0.15 dB magnitude imbalance (MI) and good matching and isolation can be observed. However, the passband selectivity is poor.

Then it can be improved by adding TZs near the passband, which is achieved by adding a pair of short-ended PCLs [2]. As shown in Fig. 4, the input impedance of short-ended PCLs Z_{ins} is calculated as:

$$Z_{ins} = j\frac{(Z_{oe1} + Z_{oo1})^2 \sin^2 \theta_2 - 4Z_{oe1}Z_{oo1}}{(Z_{oe1} + Z_{oo1}) \sin 2\theta_2} \tag{4}$$

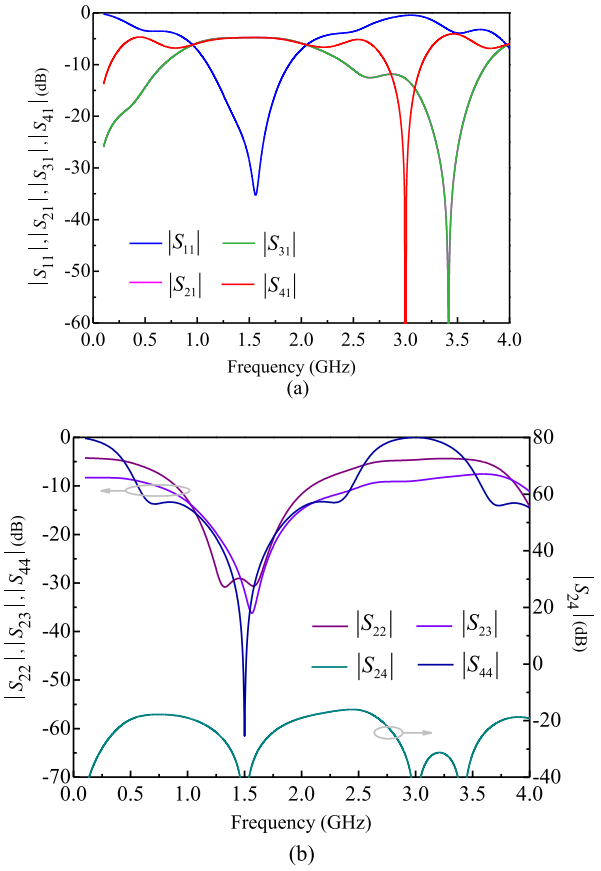

FIGURE 6. Theoretic S-parameters of the circuit in Fig. 3 without short-ended PCLs. (a) $|S_{11}|$, $|S_{21}|$, $|S_{31}|$, and $|S_{41}|$, (b) $|S_{22}|$, $|S_{23}|$, $|S_{24}|$, and $|S_{44}|$.

By imposing $Z_{ins} = 0$, the TZs positions can be derived [2]:

$$\theta_{TZ1} = \arccos\left(\frac{Z_{oe1} - Z_{oo1}}{Z_{oe1} + Z_{oo1}}\right) \tag{5a}$$
$$\theta_{TZ2} = \pi - \theta_{TZ1} \tag{5b}$$
$$\theta_{TZ3} = \pi + \theta_{TZ1} \tag{5c}$$
$$\theta_{TZ4} = \pi \tag{5d}$$

Subsequently, 1-dB FBW of wideband response can be characterized by these TZs. Fig. 7 shows the extracted FBW against Z_{oe1} and Z_{oo1}. Herein, with θ_2 chosen as 90°, Z_{ins} is equal to infinite and thus has no effects on the matching and isolation at the center frequency (CF). Then a three-way wideband FPD with CF at 1.5 GHz and 1-dB FBW of 56.67% are designed as an example, and thus $Z_{oe1} = 109\ \Omega$ and $Z_{oo1} = 33\ \Omega$ are obtained from Fig. 7.

Fig. 8 shows the theoretic response of the circuit in Fig. 3. From Fig. 8(a), the magnitude consistency is realized only at f_0. However, large magnitude imbalance (MI) of 2.82 dB away f_0 (i.e., at 1.15 and 1.85 GHz) is found. The possible reason is investigated.

As shown in Fig. 4, the input impedance Z'_{ina} and Z'_{inb} can be calculated as

$$Z'_{ina} = Z_{ina}//Z_{ins} \tag{6a}$$
$$Z'_{inb} = Z_{inb}//Z_{ins} \tag{6b}$$

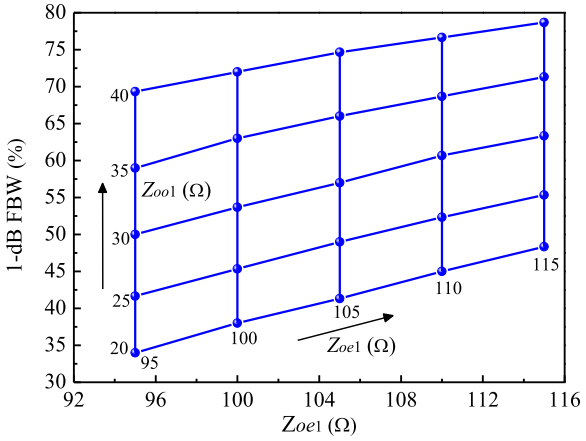

FIGURE 7. Extracted 1-dB FBW against Z_{oe1} and Z_{oo1}.

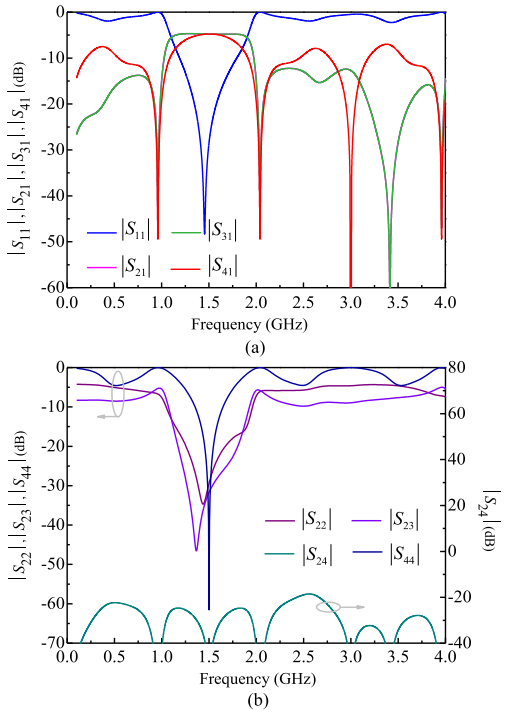

FIGURE 8. Theoretic S-parameters of the circuit in Fig. 3. (a) $|S_{11}|$, $|S_{21}|$, $|S_{31}|$, and $|S_{41}|$, (b) $|S_{22}|$, $|S_{23}|$, $|S_{24}|$, and $|S_{44}|$.

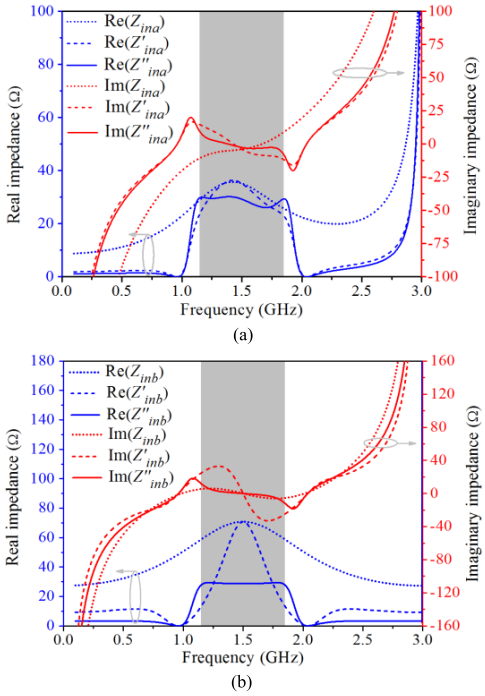

FIGURE 9. (a) Real and imaginary part of Z_{ina} and Z'_{ina}. (b) Real and imaginary part of Z_{inb} and Z'_{inb}.

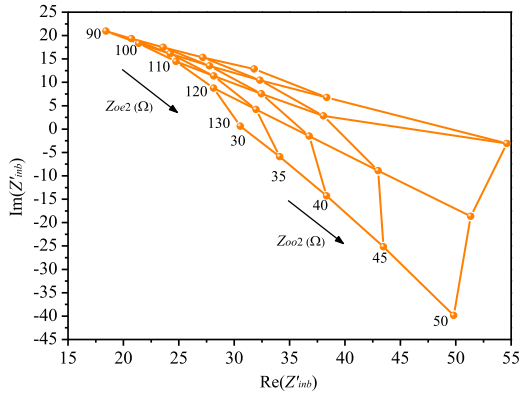

FIGURE 10. Extracted Z'_{inb} against Z_{oe2} and Z_{oo2} at 1.15 or 1.85 GHz.

Based on (3), (4), (6a), (6b), Figs. 9(a) and (b) show the calculated Z_{ina}, Z'_{ina}, Z_{inb}, and Z'_{inb}. After adding short-ended PCLs, the flatness of impedance from 1.15 to 1.85 GHz get worse, especially $\mathrm{Re}(Z'_{inb})$ for port 4. To reduce MI, Z'_{ina} and Z'_{inb} need to be more flat within the passband. According to Fig. 5, with choosing $w = 0.27$ mm and $s = 0.51$ mm, more flat Z'_{ina} (i.e., revised Z'_{ina} in Fig. 9(a)) with $\mathrm{Re}(Z'_{ina}) = 28.7\ \Omega$ and $\mathrm{Im}(Z'_{ina}) \sim 0$ are realized. To improve the flatness of Z'_{inb}, the following equations should be met

$$\mathrm{Re}(Z'_{inb})|_{f=1.15/185\ \mathrm{GHz}} = \mathrm{Re}(Z'_{inb})|_{f=1.5\ \mathrm{GHz}} \quad (7a)$$

$$\mathrm{Im}(Z'_{inb})|_{f=1.15/185\ \mathrm{GHz}} = \mathrm{Im}(Z'_{inb})|_{f=1.5\ \mathrm{GHz}} = 0 \quad (7b)$$

Similarly, Fig. 10 shows the calculated Z'_{inb} against Z_{oe2} and Z_{oo2} at 1.15 or 1.85 GHz. To meet equations (7a)-(7b), $Z_{oe2} = 111\ \Omega$ and $Z_{oo2} = 35\ \Omega$ can be obtained From Fig. 10. Then $\mathrm{Re}(Z'_{inb}) = 29.0\ \Omega$ is also realized in the passband, as shown in Fig. 9(b). Herein, after choosing proper parameters, Z''_{ina} and Z''_{inb} in Fig. 9 are the flatter inversions of Z'_{ina} and Z'_{inb}, respectively. To realize perfect matching for port 1, Z_a and Z_b can be written as

$$Z_0 = \left(Z_a^2 \Big/ Z'_{ina}\right) // \left(Z_b^2 \Big/ Z'_{inb}\right) \quad (8)$$

Subsequently, the characteristic impedances of $\lambda/4$ transformers $Z_a = 46.4\ \Omega$ and $Z_b = 65.95\ \Omega$ are calculated. Fig. 11(a) gives the corresponding response, which has perfect matching but with large MI. A tradeoff needs to be made between the matching and MI. Then by adjusting $Z_b = 108\ \Omega$ and $R_1 = 43\ \Omega$, less than 0.15 dB MI are obtained at the expense of return loss, as shown in Fig. 11(a).

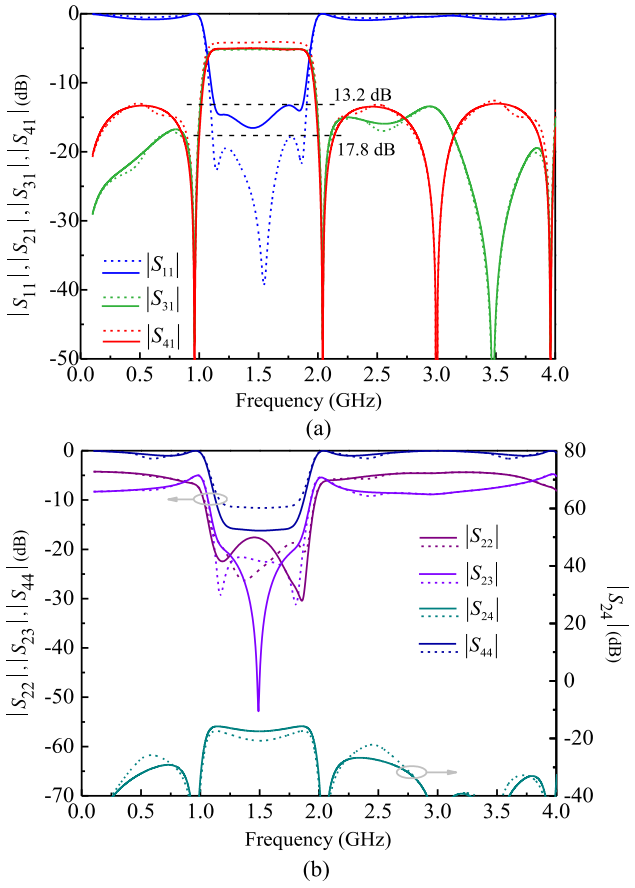

FIGURE 11. Theoretic S-parameters of the circuit in Fig. 3. (a) $|S_{11}|$, $|S_{21}|$, $|S_{31}|$, and $|S_{41}|$, (b) $|S_{22}|$, $|S_{23}|$, $|S_{24}|$, and $|S_{44}|$. (Dash: large MI; Solid: small MI).

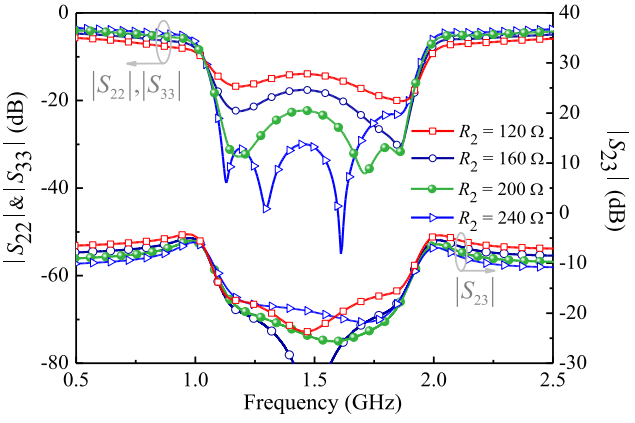

FIGURE 12. Extracted $|S_{22}|$, $|S_{23}|$, and $|S_{33}|$ against various R_2.

For the problem of phase, an equal phase can be obtained by choosing proper length of 50 Ω feeding line, which almost doesn't affect the corresponding amplitude response. R_2 is the only parameter for realizing high isolation and matching for ports 2 and 3. It can be seen that when $R_2 = 200\ \Omega$, better isolation and matching can be achieved across the operating passband. Then $R_1 = 200\ \Omega$ is chosen from Fig. 12.

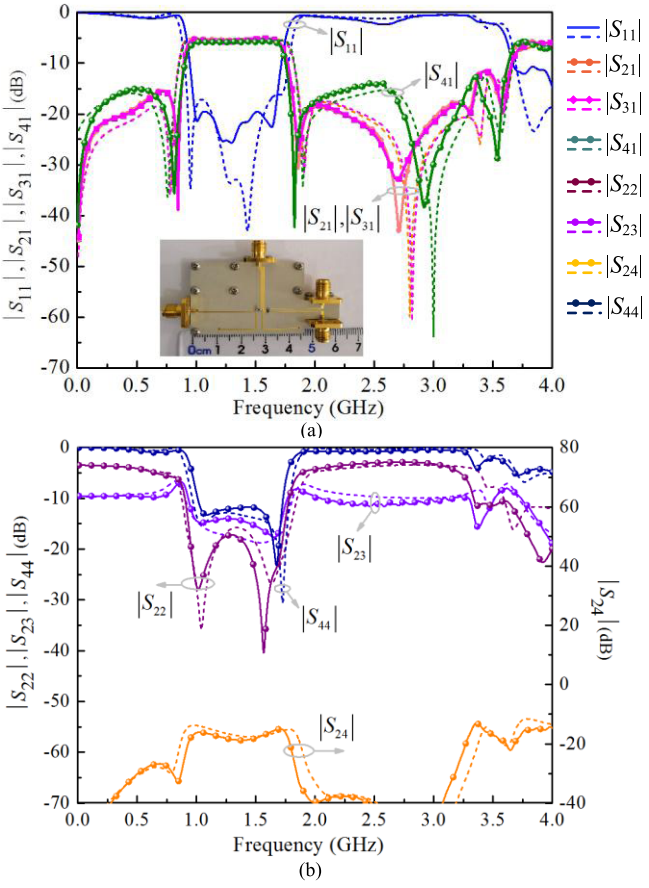

FIGURE 13. Simulated and measured results of proposed three-way FPD (a) $|S_{11}|$, $|S_{21}|$, $|S_{31}|$, and $|S_{41}|$, (b) $|S_{22}|$, $|S_{23}|$, $|S_{24}|$, and $|S_{44}|$. (Solid: Measured; Dash: EM).

The design procedure is summarized as follows: First, determine the initial parameters based on the equations (1a)-(2b); Second, choose the paprameters (Z_{oe1}, Z_{oo1}) of short-ended PCLs from Fig. 7 according to the specifications; Third, pick up the parameters (Z_{oe2}, Z_{oo2}) and (w, s) to flat the magnitude according to the equations (3), (4), (6a), (6b), (7a), (7b); Fourth, tune the parameters Z_b and R_1 to reduce ML. Last, determine R_2 from Fig. 12 to obtain good matching and isolation for port 2 and 3.

C. SIMULATED AND MEASURED RESULTS

Fig. 13(a) shows the photograph of the fabricated three-way asymmetrical FPD that has the circuit size of $0.568\lambda_g \times 0.327\lambda_g$, where λ_g is the guided-wavelength of 50 Ω microstrip line at 1.36 GHz. Fig. 13 shows the simulated and measured results of the proposed three-way FPD. In Fig. 13(a), the measured CF and 1-dB FBW are 1.36 GHz and 57.3%, respectively. The measured minimum insertion losses (ILs) and RL are better than (4.77 + 0.4) and 19.5 dB, respectively. In Fig. 13(b), the measured $|S_{22}|$, $|S_{23}|$, and $|S_{44}|$ are higher than 17.2, 14.0, and 11.6, respectively. The measured $|S_{24}|$ is better than 14.9 dB from DC to 3.33 GHz. There is some difference between the EM and

TABLE 1. Performance comparison with some reported three-way power divider.

Ref.	ILs (dB)	RLs (dB)	Number of TPs	Number of TZs	Filtering Function	Cut-off rate* (dB/MHz)	Size (λ_g^2)	Substrate
[8]	0.3	18	1	0	No	≈ 0.01	small	pHEMT
[13]	0.1	19.5	1	1	No	≈ 0.03	0.265	Microstrip
[15] Fig. 5	1.0	17	2	0	No	< 0.02	0.171	Multiplayer
[16]	1.0	16	1	0	No	< 0.02	2.24	Multiplayer
[19] Fig. 4	0.2	20	1	2	Yes	≈ 0.02	0.012	Microstrip
This work	**0.4**	**19.5**	**4**	**4**	**Yes**	**0.51**	**0.185**	**Microstrip**

Cut-off rate: $\left|\frac{A_{3dB}-A_{TZ}}{f_{3dB}-f_{TZ}}\right|$, A_{3dB}: 3-dB frequency point attenuation; A_{3dB}: TZ point attenuation; f_{3dB}: 3-dB frequency point; f_{TZ}: TZ point;

circuit response, which may be due to that the effects of open-ends, cross junctions, via holes, etc are not considered in the ideal circuit. Within the passband, the measured magnitude and phase imbalance of wideband FPD is less than 0.6 dB and 5.5° , respectively. Table 1 gives a performance comparison with some other three-way PDs. Compared with [8] based on pHEMT and [15] based on multilayer, fabrication difficulty and lower cost are obtained by using microstrip structure. Compared with [8], [13], [15], [16], [19], the proposed three-way filtering power divider features the highest number of TPs and TZs. Moreover, sharp selectivity, low insertion loss, and better return loss are also achieved in this work.

III. CONCLUSION

In this paper, an asymmetric three-way equal wideband FPD with sharp selectivity is presented. The design procedure of three-way wideband FPD is analytical developed, while the reasons and measures of large MI are also investigated. The proposed three-way PD features compact sizes, low ILs, better RLs, sharp selectivity, wideband FBW, and filtering function. The merits with good performance render it attractive for modern multifunctional communication system.

REFERENCES

[1] X. Y. Zhang, K.-X. Wang, and B.-J. Hu, "Compact filtering power divider with enhanced second-harmonic suppression," *IEEE Microw. Wireless Compon. Lett.*, vol. 23, no. 9, pp. 483–485, Sep. 2013.

[2] H. Zhu, A. M. Abbosh, and L. Guo, "Wideband four-way filtering power divider with sharp selectivity and wide stopband using looped coupled-line structures," *IEEE Microw. Wireless Compon. Lett.*, vol. 26, no. 6, pp. 413–415, Jun. 2016.

[3] Y. L. Wu, Z. Zhuang, G. Y. Yan, Y. A. Liu, and Z. Ghassemlooy, "Generalized dual-band unequal filtering power divider with independently controllable bandwidth," *IEEE Trans. Microw. Theory Techn.*, vol. 65, no. 10, pp. 3838–3848, Oct. 2017.

[4] F. Lin, Q.-X. Chu, Z. Gong, and Z. Lin, "Compact broadband Gysel power divider with arbitrary power-dividing ratio using microstrip/slotline phase inverter," *IEEE Trans. Microw. Theory Techn.*, vol. 60, no. 5, pp. 1226–1234, May 2012.

[5] W. Feng, Y. Zhao, W. Che, R. Gómez-García, and Q. Xue, "Single-ended-to-balanced filtering power dividers with wideband common-mode suppression," *IEEE Trans. Microw. Theory Techn.*, vol. 66, no. 12, pp. 5531–5542, Dec. 2018.

[6] C. Zhu, J. Xu, W. Kang, and W. Wu, "Microstrip multifunctional reconfigurable wideband filtering power divider with tunable center frequency, bandwidth, and power division," *IEEE Trans. Microw. Theory Techn.*, vol. 66, no. 6, pp. 2800–2813, Jun. 2018.

[7] R. Gómez-García, D. Psychogiou, and D. Peroulis, "Fully-tunable filtering power dividers exploiting dynamic transmission-zero allocation," *Microw., Antennas Propag.*, vol. 11, no. 3, pp. 378–385, Mar. 2017.

[8] Y. A. Lai, C. M. Lin, J. C. Chiu, C. H. Lin, and Y. H. Wang, "A compact Ka-band planar three-way power divider," *IEEE Microw. Wireless Compon. Lett.*, vol. 17, no. 12, pp. 840–842, Dec. 2007.

[9] Y. Wu, Y. Liu, Q. Xue, S. Li, and C. Yu, "Analytical design method of multiway dual-band planar power dividers with arbitrary power division," *IEEE Trans. Microw. Theory Techn.*, vol. 58, no. 12, pp. 2832–2841, Dec. 2010.

[10] X. Wang, I. Sakagami, K. Takahashi, and S. Okamura, "A planar three-way dual-band power divider using two generalized open stub Wilkinson dividers," in *Proc. Asia–Pacific Microw. Conf.*, Dec. 2010, pp. 714–717.

[11] I. Sakagami, X. Wang, K. Takahashi, and S. Okamura, "Generalized two-way two-section dual-band Wilkinson power divider with two absorption resistors and its miniaturization," *IEEE Trans. Microw. Theory Techn.*, vol. 59, no. 11, pp. 2833–2847, Nov. 2011.

[12] A. A. Alshehri, S. M. Alsaif, A. Alshehry, H. Alsuraisry, H. M. Behairy, and R.-B. Wu, "Three-way cascade power divider and combiner for satellite communications," in *Proc. IEEE Wireless Power Transf. Conf. (WPTC)*, May 2017, pp. 1–4.

[13] J. C. Chiu, J. M. Lin, and Y. H. Wang, "A novel planar three-way power divider," *IEEE Microw. Wireless Compon. Lett.*, vol. 16, no. 8, pp. 449–451, Aug. 2006.

[14] A. M. Abbosh, "A compact UWB three-way power divider," *IEEE Microw. Wireless Compon. Lett.*, vol. 17, no. 8, pp. 598–600, Aug. 2007.
[15] A. M. Abbosh, "Design of ultra-wideband three-way arbitrary power dividers," *IEEE Trans. Microw. Theory Techn.*, vol. 56, no. 1, pp. 194–201, Jan. 2008.
[16] A. M. Abbosh, "Three-way parallel-coupled microstrip power divider with ultrawideband performance and equal-power outputs," *IEEE Microw. Wireless Compon. Lett.*, vol. 21, no. 12, pp. 649–651, Dec. 2011.
[17] C. Feng, G. Zhao, X.-F. Liu, and F.-S. Zhang, "Planar three-way dual-frequency power divider," *Electron. Lett.*, vol. 44, no. 2, pp. 133–134, Jan. 2009.
[18] W. Choe and J. Jeong, "Compact modified Wilkinson power divider with physical output port isolation," *IEEE Microw. Wireless Compon. Lett.*, vol. 24, no. 12, pp. 845–847, Dec. 2014.
[19] P. K. Singh, S. Basu, and Y. H. Wang, "Coupled line power divider with compact size and bandpass response," *Electron. Lett.*, vol. 45, no. 17, pp. 892–894, Aug. 2009.
[20] L. I. Parad and R. L. Moynihan, "Split-tee power divider," *IEEE Trans. Microw. Theory Techn.*, vol. MTT-13, no. 1, pp. 91–95, Jan. 1965.
[21] Y. Wu, Y. Liu, Y. Zhang, J. Gao, and H. Zhou, "A dual band unequal Wilkinson power divider without reactive components," *IEEE Trans. Microw. Theory Techn.*, vol. 57, no. 1, pp. 216–222, Jan. 2009.
[22] R. Mirzavand, M. M. Honari, A. Abdipour, and G. Moradi, "Compact microstrip Wilkinson power dividers with harmonic suppression and arbitrary power division ratios," *IEEE Trans. Microw. Theory Techn.*, vol. 61, no. 1, pp. 61–68, Jan. 2013.
[23] V. K. Tripathi, "On the analysis of symmetrical three-line microstrip circuits," *IEEE Trans. Microw. Theory Techn.*, vol. MTT-25, no. 9, pp. 726–729, Sep. 1977.

CHUANMING ZHU received the Ph.D. degree in information and communication engineering from the Nanjing University of Science and Technology, Nanjing, China, in 2018. His current research interests include microwave passive components and multifunctional integrated circuits. He is a Reviewer of several international journals, including the IEEE Transactions and Letters.

JIAN ZHANG received the B.Eng. degree from Southeast University, Nanjing, China, in 1999, and the Ph.D. degree from the Shanghai Institute of Microsystem and Information Technology, Chinese Academy of Sciences (CAS), Shanghai, China, in 2008. From 1999 to 2002, he was an Engineer with the Wuhan Research Institute of Post and Tele-communication, Wuhan, China, where he was involved in the circuits design for ATM-PON access network application. From 2008 to 2010, he was a Post-Doctoral Researcher with the Microwave Electronics Laboratory, Department of Microtechnology and Nanoscience (MC2), Chalmers University of Technology, Götebörg, Sweden, where he was engaged in monolithic microwave integrated circuit (MMIC) development. From 2010 to 2012, he was a Marie Curie Experienced Researcher with the High Frequency Electronic Circuits Division, Institute of Electronics and Communications and Information Technology (ECIT), Queens University of Belfast, Belfast, U.K., where he was involved in the development of MMIC and communication systems for wireless personal area network (WPAN) applications using SiGe process technology. In 2012, he returned to the Shanghai Institute of Microsystem and Information Technology, CAS. Since 2017, he has been with Hangzhou Dianzi Unversity. His main research interest includes MMIC and passive circuit designs for millimeter-wave communication and applications.